Published in final edited form as:
J Cell Sci. 2005 April 15; 118(Pt 8): 1745–1755.

Assembly pathway of the anastral *Drosophilaoocyte* meiosis I spindle

Helén Nilsson Sköld[*], **Donald J. Komma**, and **Sharyn A. Endow**[‡]
Department of Cell Biology, Duke University Medical Center, Durham, NC 27710, USA

Summary

Oocyte meiotic spindles of many species are anastral and lack centrosomes to nucleate microtubules. Assembly of anastral spindles occurs by a pathway that differs from that of most mitotic spindles. Here we analyze assembly of the *Drosophila* oocyte meiosis I spindle and the role of the Nonclaret disjunctional (Ncd) motor in spindle assembly using wild-type and mutant Ncd fused to GFP. Unexpectedly, we observe motor-associated asters at germinal vesicle breakdown that migrate towards the condensed chromosomes, where they nucleate microtubules at the chromosomes. Newly nucleated microtubules are randomly oriented, then become organized around the bivalent chromosomes. We show that the meiotic spindle forms by lateral associations of microtubule-coated chromosomes into a bipolar spindle. Lateral interactions between microtubule-associated bivalent chromosomes may be mediated by microtubule crosslinking by the Ncd motor, based on analysis of fixed oocytes. We report here that spindle assembly occurs in an *ncd* mutant defective for microtubule motility, but lateral interactions between microtubule-coated chromosomes are unstable, indicating that Ncd movement along microtubules is needed to stabilize interactions between chromosomes. A more severe *ncd* mutant that probably lacks ATPase activity prevents formation of lateral interactions between chromosomes and causes defective microtubule elongation. Anastral *Drosophila* oocyte meiosis I spindle assembly thus involves motor-associated asters to nucleate microtubules and Ncd motor activity to form and stabilize interactions between microtubule-associated chromosomes during the assembly process. This is the first complete account of assembly of an anastral spindle and the specific steps that require Ncd motor activity, revealing new and unexpected features of the process.

Keywords

Meiotic spindle assembly; Anastral spindles; Microtubule motor; Ncd; Live oocytes

Introduction

Assembly of normal bipolar spindles is essential for accurate chromosome distribution during cell division. Work over more than a century (for a review, see Mitchison and Salmon, 2001) has greatly advanced our knowledge of mitotic processes, including the mechanism of mitotic spindle assembly. Recent major advances have been the remarkable development of in vitro spindle assembly assays (Heald et al., 1996), the innovation of new fluorescence methods to follow spindle dynamics (Desai et al., 1998; Waterman-Storer et al., 1998), and the discovery of microtubule motors and their roles in the mitotic apparatus (Inoué and Salmon, 1995; Endow, 1999; Hunter and Wordeman, 2000; Sharp et al., 2000). Motors of the kinesin family, together with cytoplasmic dynein, are now thought to be essential in assembling and organizing bipolar

‡Author for correspondence (e-mail: endow001@mc.duke.edu).
*Present address: Kristineberg Marine Research Station, Royal Swedish Academy of Sciences, Kristineberg 2130, S-450 34 Fiskebäckskil, Sweden

mitotic spindles. Despite recent progress, basic aspects of mitotic spindle assembly and function, such as the relationship between microtubule dynamics and spindle mechanics, are not yet fully understood and are actively being investigated (Karsenti and Vernos, 2001).

Much less is known about meiotic spindles, particularly those of oocytes, which differ in different organisms (Wilson, 1934). Strikingly, oocyte spindles of many species are anastral and lack centrosomes, despite their bipolar structure. Mouse oocyte meiotic spindles are not associated with centrioles (Szollosi et al., 1972), but centrosomal proteins such as γ-tubulin and pericentrin are localized in patches at their broad spindle poles (Combelles and Albertini, 2001; Gueth-Hallonet et al., 1993; Lee et al., 2000; Carabatsos et al., 2000; Doxsey et al., 1994). Other oocyte spindles have been reported to lack centrosomal proteins. The *Drosophila* oocyte meiosis I spindle is a classical example of an anastral spindle in which centrosomal proteins such as γ-tubulin and CP60 have not been detected (Matthies et al., 1996); these proteins have been localized to the central spindle pole body that lies between the two oocyte meiosis II spindles, but not to the distal spindle poles, which are thought to be retained from the meiosis I spindle (Riparbelli and Callaini, 1996; Endow and Komma, 1998; Riparbelli and Callaini, 1998; Brent et al., 2000). More recently, two conserved centrosomal proteins, Msps and DTACC, have been found at the poles of the *Drosophila* oocyte meiosis I spindle, where they have been proposed to stabilize the poles after assembly and maintain spindle bipolarity (Cullen and Ohkura, 2001). These two microtubule-associated proteins may form a complex in oocytes similar to that reported in mitotic cells (Lee et al., 2001).

The mechanism by which spindles assemble in the absence of centrosomes is still not well understood. Mutants of the *Drosophila* Ncd motor protein, a member of the Kinesin-14 (formerly C-terminal motor) (Lawrence et al., 2004) group of kinesin proteins, form highly aberrant oocyte meiosis I spindles, implying an essential role for the motor in normal spindle assembly. The minus-end Ncd motor has been proposed to function in spindle assembly by crosslinking microtubules and moving along microtubules to the minus ends, focusing the ends into poles (Hatsumi and Endow, 1992a; Hatsumi and Endow, 1992b; Matthies et al., 1996). The microtubule crosslinking activity of Ncd could hold the spindle-associated bivalent chromosomes together laterally (Hatsumi and Endow, 1992a), and replace centrosomes in the oocyte meiosis I spindles by providing microtubule organizing activity required for pole formation (Hatsumi and Endow, 1992b; Hatsumi and Endow, 1992a; Matthies et al., 1996) and interacting with Msps and D-TACC at the spindle poles (Cullen and Ohkura, 2001). This model of anastral spindle pole formation is supported by the formation of aster-like foci when taxol-stabilized microtubules are mixed with motors in vitro (Surrey et al., 2001). Asters formed from microtubules mixed with Kinesin-1 (formerly conventional kinesin) (Lawrence et al., 2004), a plus-end motor, have plus ends at the center, whereas asters formed from microtubules mixed with minus-end Ncd have minus ends at the center. Crosslinking and lateral organization of microtubules following aster formation could result in assembly of a bipolar spindle.

This model helps to explain the role of the Ncd motor in anastral spindle assembly in *Drosophila* oocytes, but it is largely incomplete and lacks several basic features: it does not address a key question of how microtubules are nucleated for spindle assembly in *Drosophila* oocytes, a process that has been proposed to involve nucleation at chromatin in *Xenopus* oocytes (Heald et al., 1996), and omits intermediate steps in the assembly process that are needed to fully understand spindle assembly. Here we report new findings regarding nucleation of microtubules and the role of the Ncd motor in *Drosophila* oocyte meiosis I spindle assembly that compel modification of models for spindle assembly based on previous work (Hatsumi and Endow, 1992a; Hatsumi and Endow, 1992b; Matthies et al., 1996).

Materials and Methods

Drosophilastocks

Oocytes were from females homozygous for ca^{nd}, an *ncd* null mutant deleted for the promoter and 5′ end of the coding region (Yamamoto et al., 1989), and transgenic for wild-type or mutant *ncd* fused to *Aequorea victoria* S65T *gfp* (Heim et al., 1995), denoted *gfp**. Controls had two or four copies of wild-type *ncdgfp** (line *4121: M3M1/SM5; M9F1/TM3* or *M3M1; M9F1* females) (Endow and Komma, 1996; Endow and Komma, 1997), which we showed previously rescues ca^{nd} for chromosome mis-segregation and embryo inviability (Endow and Komma, 1996). The requirement for motor movement on microtubules was examined using *ncdNKgfp** (*M5M2*), a motor that binds tightly to microtubules in vitro but does not move on microtubules in gliding assays (Song and Endow, 1998). Oocytes of $ncd^{2}gfp^{*}$ (*M8M3*) females carrying a severe loss-of-function *ncd* allele with genetic effects on chromosome segregation similar to ca^{nd} (O'Tousa and Szauter, 1980; Endow and Komma, 1996; Endow and Komma, 1997) were examined for comparison. We also analyzed oocytes of $fs(2)TW1^{APL10}$ females (referred to as *APL10*) carrying an EMS-induced maternal-effect female-sterile mutation of the maternally expressed γ-tubulin gene at 37C (Schüpbach and Wieshaus, 1989) (a gift of T. Schüpbach), together with ca^{nd} and three or four copies of *ncdgfp**. Chromosome behavior was analyzed in *histone2A-gfp* oocytes (Clarkson and Saint, 1999) (a gift of R. Saint).

Molecular tests

Tests of *ncdgfp** (line *4121*) ca^{nd} and *ncdNKgfp** (*M5M2*) ca^{nd} flies were carried out to confirm the presence of the transgene and absence of genomic *ncd* genes. PCR was performed on DNA from homozygous transgenic females using primers that flank an intron in *ncd*. The PCR fragment produced by the *ncd* cDNA transgene was 572 bp compared to 632 bp by genomic *ncd*. One primer was in the deleted region of ca^{nd}, thus ca^{nd} did not produce a PCR product. Tests of *ncdgfp** (line *4121*) and *ncdNKgfp** (*M5M2*) each showed a single band of the correct size for the transgene. DNA sequence analysis of the *ncdNKgfp** (*M5M2*) PCR fragment showed the correct mutational change of N600K and no other nucleotide changes in the sequenced region. The molecular tests thus confirmed the two lines as carrying the *ncd* transgene with no genomic *ncd* gene.

Genetic tests

Genetic tests of *ncdNKgfp** females were performed as described previously (Komma et al., 1991). Briefly, *ncdNKgfp** or *ncdNKgfp**/+ females were mated to tester males ($y^{2}w^{bf}/B^{S}Y$, $y/B^{S}Y$, $+/B^{S}Y$ or $+/B^{S}Y^{+}$) and offspring were monitored for gametic and early zygotic X chromosome segregation. Exceptional X/X/Y and X/0 offspring were attributed to gametic chromosome nondisjunction and loss, and gynandromorphs to early zygotic chromosome loss. Minute offspring, caused by loss of chromosome 4, were entered into calculations of embryo viability, but were omitted from estimates of chromosome nondisjunction and loss owing to their variable recovery. Frequencies of gametic and zygotic chromosome mis-segregation were calculated as described (Komma et al., 1991). Genetic tests have been reported previously for the *ncdgfp** and $ncd^{2}gfp^{*}$ transgenes (Endow and Komma, 1996; Endow and Komma, 1997).

Time-lapse laser-scanning confocal microscopy

Oocytes were prepared by hand-dissecting egg chambers from ovaries of 3- to 5-day-old females in Schneider's *Drosophila* medium (GIBCO, Grand Island, NY) supplemented with 10–15% heat-inactivated fetal calf serum. Oocytes were cultured for short periods of time at room temperature as described (Dorman et al., 2004) to image meiosis I spindle assembly. Briefly, stage 12 and 13 oocytes (Foe et al., 1993) were carefully transferred to a ~30 μl drop of Schneider's medium on an oxygen-permeable Teflon membrane (YSI, Yellow Springs, OH)

supported by a custom metal slide (Davis et al., 1995). A thin ring of vacuum grease, extruded through a 16-gauge needle, was used to support a glass coverslip placed over the oocytes. Wild-type oocytes cultured at room temperature in the chambers completed germinal vesicle breakdown and meiosis I spindle assembly in ~40 minutes. Oocytes were imaged using a Zeiss Axioskop with a 63× 1.4 NA Planapochromat objective and Bio-Rad MRC 600 laser-scanning confocal system equipped with a custom filter set optimized for GFP (Endow and Komma, 1996; Endow and Komma, 1997). Time-lapse images were collected at 30-second intervals and 2.5× zoom using COMOS software, beginning at germinal vesicle breakdown, and analyzed using NIH Image version 1.62.

Fixation and staining of oocytes

Oocytes were fixed and stained with rhodamine-conjugated anti-α-tubulin antibody (a gift of W. Sullivan) and DAPI, as reported previously (Endow and Komma, 1997). Images of chromosomes were collected using a Leica Dialux 22 fluorescence microscope and a 63× 1.4 NA Planapochromat objective with a Princeton Instruments PentaMax-1317-K cooled CCD camera and IPLab Spectrum software. The cooled CCD images were overlaid on images of spindles collected with the Bio-Rad MRC 600 confocal system, as described (Endow and Komma, 1997), using Adobe Photoshop version 8.0.

Digital images

Images were cropped and assembled into montages using NIH Image. Montages were saved as TIFF files and opened in Adobe Photoshop for resizing, final changes in resolution, and adjustments to brightness, contrast and color. All adjustments were linear and applied to the entire image.

Fluorescence loss in photobleaching

Fluorescence loss in photobleaching (FLIP) experiments (Cole et al., 1996) were performed by repeatedly scanning a defined region in a meiotic spindle of wild-type (two-dose *M3M1 ncdgfp*; ca*nd) or mutant (*M5M2 ncdNKgfp* ca*nd) oocytes using a Bio-Rad Radiance2100 confocal system equipped with a 63× 1.4 NA Planapochromat objective. Three pre-bleach images of the spindle were recorded at 3× zoom and 20% laser power, then thirty scans were performed at 1.6-second intervals at 100% laser power in a 12×24 pixel region of the spindle and 20% outside the ROI, followed by 15 scans of the spindle at 20% laser power. Images were recorded after each scan to monitor fluorescence loss. The mean grey-level pixel value of a defined area within the ROI was determined over time and values were plotted as a function of time. Curves were fitted to a single exponential equation, $y=m_3+m_2*e^{(-m1*M0)}$, where y=grey-level value, M_0=time (seconds) and $y=m_3+m_2$ at t=0, using Kaleidagraph version 3.6.2. The dissociation rate ($k_d=m_1$) for loss of fluorescence was obtained from the curve fit.

Results

Meiosis I spindle assembly in live oocytes

A transgene expressing the *Drosophila* Ncd motor fused to a bright variant of GFP, S65T GFP (Heim et al., 1995), denoted GFP*, was used to visualize microtubules during nucleation, elongation and assembly of the oocyte meiosis I spindle following germinal vesicle breakdown. In previous studies, we found that NcdGFP* binds to spindle microtubules and can be used to visualize mature oocyte meiosis I spindles and assembly of meiosis II spindles (Endow and Komma, 1997; Endow and Komma, 1998), as well as mitotic spindles of early embryos (Endow and Komma, 1996). Because the timing of Ncd expression in oocytes and that required for GFP* folding are not known, it was not certain that NcdGFP* could be used to follow meiosis I spindle assembly. Unexpectedly, we have recently been able to visualize germinal vesicle

breakdown, microtubule nucleation, and assembly of the meiosis I spindle using NcdGFP* bound to microtubules in immature, late stage 13 oocytes.

We first examined oocytes from females expressing four copies of *ncdgfp** in the genetic background of the *ncd* deletion null mutant, claret nondisjunctional (ca^{nd}). These females appear wild type and previously reported genetic tests showed that they are fully rescued for the mutant effects of ca^{nd} on meiotic and mitotic chromosome distribution (Endow and Komma, 1996). We found that NcdGFP* is present in the germinal vesicle of *ncdgfp** oocytes, giving a uniform fluorescence (Fig. 1A,B). The first signs of germinal vesicle breakdown are an unevenness to the nuclear envelope (Fig. 1A, arrowhead), followed by distortion of large regions of the margin (Fig. 1B) and dispersion of NcdGFP* fluorescence into the ooplasm (Fig. 1C). A dark body that excludes NcdGFP* is present within the germinal vesicle (Fig. 1A, arrow) and was tentatively identified as the karyosome of condensed oocyte meiotic chromosomes, or endobody. It is this body around which the oocyte meiosis I spindle forms.

Following germinal vesicle breakdown, NcdGFP* binds to microtubules that form the spindle, permitting the steps of assembly to be visualized by time-lapse imaging. Small fluorescent foci or asters appear in or around the germinal vesicle at the time of its breakdown (Fig. 1C,D, arrows). One or more of these asters migrates through the dispersing nucleoplasm towards the endobody and associates with it. Shortly thereafter, fluorescent spikes or bundles of NcdGFP* motor-decorated microtubules can be observed projecting randomly from the outer surface of the karyosome (Fig. 1E). The microtubules elongate, forming a star-like cluster with the karyosome at the center (Fig. 1F,G), then assemble around separated dark masses (Fig. 1H), which, based on fixed specimens stained for DNA (Endow and Komma, 1997), correspond to the bivalent chromosomes. The microtubule-associated chromosomes are separate from one another, rather than forming a single mass, as reported by others (Matthies et al., 1996). We then observe, for the first time, that the microtubule-associated structures associate laterally with one another (Fig. 1I) and elongate to form a bipolar spindle (Fig. 1J-L). The time-lapse sequence can be viewed as a movie (Supplementary material, Movie 1).

Spindle assembly was analyzed in oocytes with two or four copies of *ncdgfp**. No significant differences in the kinetics of spindle assembly or structure of mature spindles were observed between the two- and four-dose *ncdgfp** oocytes; the data are therefore grouped together in Table 1. Time-lapse imaging showed that assembly of a bipolar meiosis I spindle requires 40.0 ±1.6 minutes following germinal vesicle breakdown or 29.4±1.6 minutes following microtubule nucleation in two- or four-dose *ncdgfp** oocytes (n=10). The association of fluorescent foci with the endobody occurred at 9.9±1.3 minutes following germinal vesicle breakdown and lateral interactions of microtubule-associated structures were observed at 22.4 ±2.9 minutes (Table 1). In some oocytes, the bipolar spindle in the final stages of assembly rotated around the axis formed by its poles, as observed previously for mature *Drosophila* oocyte meiosis I spindles (Endow and Komma, 1997).

Chromosomes in live oocytes

Chromosome behavior during meiosis I spindle assembly has previously only been described using fixed material (e.g. Theurkauf and Hawley, 1992). Here we report chromosome behavior using exclusion of NcdGFP* to infer the position of the chromosomes in spindles of live oocytes. When analyzing the spindle, clearly discernable dark spots can be observed that we interpret to be the condensed meiotic chromosomes, based on staining of fixed oocytes (Endow and Komma, 1997) (Fig. 2). The chromosomes exclude NcdGFP* and appear dark by fluorescence imaging. At the time of germinal vesicle breakdown, the chromosomes are condensed in the endobody (Fig. 1A,B). After association with one or more NcdGFP*-containing fluorescent asters (Fig. 1C,D), microtubules nucleate around the endobody (Fig. 1E), forming spikes or unfocused bundles (Fig. 1F,G). Separate dark spots representing the

three large *D. melanogaster* bivalent chromosomes then differentiate, ensheathed by microtubules (Fig. 1H), associate laterally (Fig. 1I) and elongate into a bipolar spindle (Fig. 1J-L).

Following the appearance of a bipolar spindle, the chromosomes often moved out from the spindle center and then back towards the metaphase-arrest position at the center (Sonnenblick, 1950). Even after attaining this position, the chromosomes could still be seen moving within the spindle. An example of chromosome movement after appearance of a bipolar spindle is shown in images taken from a time-lapse sequence of the same oocyte as shown in Fig. 1. The dark spots corresponding to the large chromosomes move together, then apart, rather than remaining in a fixed position in the spindle (Fig. 3; Supplementary material, Movie 2). This behavior was also observed in other oocytes after the appearance of a bipolar spindle.

We also imaged oocytes expressing histone2A-GFP, in which the chromosomes were clearly labeled by fluorescence and a (usually) dark spindle profile could be seen by exclusion of the high background of fluorescent particles (Supplementary material, Fig. S1). Time-lapse imaging of *histone2A-gfp* oocytes (Supplementary material, Movie 3) showed behavior of the chromosomes that was similar to the dark spots that we attribute to being the chromosomes in *ncdgfp** oocytes: after germinal vesicle breakdown, the histone2A-GFP labeled endobody differentiated into bivalent chromosomes. Lateral interactions formed between the chromosomes, then the chromosomes moved in various directions during spindle formation and finally appeared together in the center of the spindle. Movements of the chromosomes continued after the apparent appearance of a bipolar spindle; the chromosomes did not remain oriented in a defined position on the spindle, even after attaining a metaphase-arrest position. Further studies using specific fluorescent kinetochore or chromosome labels could provide information regarding chromosome pairing and alignment on the spindle during assembly, and at earlier times of meiosis. These studies may answer longstanding questions regarding chromosome pairing behavior during meiosis in *Drosophila* oocytes (Grell, 1962; Grell, 1964; Novitski, 1964).

Spindle assembly in *ncdNKgfp** mutant oocytes

To determine the role of Ncd motility in meiosis I spindle assembly, we examined the effects of a mutant, NcdNK, which blocks Ncd motor movement on microtubules. The NcdNK protein hydrolyzes ATP at a basal level, but binds tightly to microtubules in vitro and shows no microtubule-activated ATPase activity, which is essential for motor movement along microtubules, and, consequently, shows no motility in microtubule gliding assays (Song and Endow, 1998).

The *ncdNK* mutant, when tested genetically as a fusion to *gfp**, showed high frequencies of chromosome mis-segregation and embryo inviability (Table 2), effects that parallel the severe loss-of-function mutant, ncd^2gfp* (Endow and Komma, 1997), and null mutant, ca^{nd} (Table 2). The frequency of gametic nondisjunction and loss (0.138) caused by the *ncdNKgfp** mutant was higher than zygotic loss (0.040), but both frequencies were lower than for ca^{nd} (0.238 and 0.056, respectively). The low viability of *ncdNKgfp** ca^{nd} embryos (0.097) was comparable to that of ca^{nd} embryos (0.113). The mutant thus showed loss of function for meiotic and early mitotic chromosome distribution, and embryo inviability. No dominant effects on chromosome segregation were observed in tests of heterozygous *ncdNKgfp** $ca^{nd}/+$ females, however, the females produced a significantly lower frequency of viable embryos (0.789) than wild-type *ncdgfp** ca^{nd} females (0.930) (Table 2), indicating a dominant effect of the transgene on embryo viability.

Based on analysis of time-lapse sequences of live oocytes, the major effect of the *ncdNKgfp** mutant on meiosis I spindle assembly was to cause defective lateral interactions between

microtubule-associated bivalent chromosomes, prolonging the time required to form a bipolar spindle. Nucleation of microtubules prior to spindle assembly occurred at 9.9±3.8 minutes (*n*=4) following the end of germinal vesicle breakdown, the same as for wild-type *ncdgfp** (Table 1). However, the time required to establish lateral interactions between spindle-associated chromosomes was variable, and the interactions were unstably formed or failed to form (Table 1).

Several examples of spindles from mature *ncdNKgfp** oocytes are shown in Fig. 4, illustrating the major defect of the mutant in establishing stable lateral interactions between spindle-associated bivalent chromosomes, which are necessary for the chromosomes to form a single bipolar spindle. The cumulative effect was to produce spindles in which one or more of the component spindles was separated from the rest (Fig. 4A), split spindles (Fig. 4A,B), or side-by-side partially merged spindles (Fig. 4C-E). An apparently normal spindle is shown (Fig. 4F) in an *ncdNKgfp** oocyte which was not followed over time, however, the time-lapsed spindles typically showed separated or unstable spindles in which the component spindles moved together, then apart.

Spindle assembly in *ncd^{2}gfp** mutant oocytes

For comparison, we examined oocytes of *ncd^{2}gfp** females, mutant for a severe loss-of-function *ncd* allele that resembles the deletion null mutant, *cand*, in its genetic effects (O'Tousa and Szauter, 1980; Endow and Komma, 1996; Endow and Komma, 1997). The in vitro motility characteristics of Ncd^2 have not been examined because of insolubility of the bacterially-expressed protein, but the location and nature of the mutational change in the motor domain indicate a defect in nucleotide binding or release, which probably affects both the basal and microtubule-stimulated ATPase of the motor (Endow and Komma, 1997).

The cytological effects that we observed were more severe in *ncd^{2}gfp** than *ncdNKgfp** oocytes. Germinal vesicles of *ncd^{2}gfp** oocytes were dark rather than fluorescent, as in wild-type *ncdgfp** or *ncdNKgfp** oocytes, indicating that the mutant motor is excluded from the oocyte nucleus. Germinal vesicle breakdown allowed the Ncd^{2}GFP* motor to interact with the endobody. Association of fluorescent asters with the karyosome occurred at 12.8±1.8 minutes (*n*=5) following completion of germinal vesicle breakdown, not significantly longer than for wild-type oocytes. However, lateral interactions of the spindle-associated chromosomes do not form or are greatly delayed compared to wild-type oocytes (Table 1), thus normal bipolar spindles do not assemble in the *ncd^{2}gfp** oocytes (Supplementary material, Movie 4). This is the first report identifying the specific step in anastral spindle assembly that is defective in a severe loss-of-function *ncd* mutant. The mean time of observation from the end of germinal vesicle breakdown or initiation of microtubule nucleation was >129.5±9.9 minutes or >116.7 ±10.8 minutes, respectively. Spindle assembly in *ncd^{2}gfp** oocytes thus takes more than three to four times as long as in wild-type *ncdgfp** oocytes owing to the failure of lateral interactions to form between microtubule-coated chromosomes, and does not result in a bipolar spindle.

The spindles in *ncd^{2}gfp** oocytes were abnormal, consisting of separated or side-by-side spindles, rather than normal bipolar spindles (Fig. 5). Some spindles appeared immature, as if they had not progressed beyond the initial stages of assembly (Fig. 5A), whereas others consisted of multiple, small separated spindles (Fig. 5B-E), indicating that elongation of microtubules associated with chromosomes was defective, as well as formation of lateral interactions between microtubule-associated chromosomes. Normal bipolar spindles were not observed in *ncd^{2}gfp** oocytes.

Fluorescent aster and meiosis I spindle assembly

A striking feature of the assembly pathway we report here is the observation of fluorescent foci or asters that associate with the karyosome of condensed chromosomes and nucleate microtubules in the initial stages of spindle formation. The fluorescence of the asters indicates that they contain NcdGFP*, which is probably associated with microtubules. The asters were especially prominent in *ncdNKgfp** oocytes, where six out of ten oocytes examined at the time of germinal vesicle breakdown showed larger than usual asters (Fig. 6A), compared to wild-type *ncdgfp** oocytes (Fig. 1C,D), including one oocyte that contained a large number of asters, several of which moved towards the endobody as germinal vesicle breakdown progressed (Fig. 6B).

There was no apparent specific place of aster formation. They either appeared first in the oocyte cytoplasm and migrated into the germinal vesicle after breakdown or they appeared in the nucleoplasm and migrated towards the endobody. The asters disappeared just prior to the appearance of newly nucleated microtubules at the endobody. The observation that microtubules appear to nucleate from the asters raises the possibility that they bring nucleating substance to the endobody.

The apparent nucleation of microtubules at the endobody by the asters suggested that they might contain γ-tubulin. To examine this idea, we analyzed oocytes of a γ-Tub37C mutant, *APL10*, produced by *APL10*/+ heterozygous or *APL10* homozygous females carrying ca^{nd} and three or four copies of *ncdgfp**. *APL10* affects the maternally expressed γ-tubulin at cytological map position 37C, which is present in oocytes and early embryos of *Drosophila* (Tavosanis et al., 1997). Nine of 16 *APL10*/+ oocytes (Fig. 6C) and seven out of eight *APL10* oocytes showed prominent asters at the time of germinal vesicle breakdown, like the *ncdNKgfp** oocytes. Most of the meiosis I spindles of *APL10*/+ oocytes (8 of 11) or *APL10* oocytes (11 of 13) were normal. The abnormal spindles showed only small differences from normal spindles: side-by-side or slipped spindles or slightly split poles, indicating that the *APL10* γ- tubulin mutant has only slight effects on meiosis I spindle assembly and maintenance in oocytes.

The basis of its effect on asters may be that the *APL10* mutant allele contains a missense mutation of Glu116 to Arg (Wilson and Borisy, 1998) that lies in a region of γ-tubulin corresponding to helix H3 of α/β-tubulin (Nogales et al., 1998). Helix H3 of α/β-tubulin is present in microtubules at the interface between two protofilaments, suggesting that the *APL10* mutation may affect lateral interactions between γ-tubulin molecules. The substitution of a positively charged residue, Arg, with a negatively charged residue, Glu, could increase interactions between γ-tubulin molecules. This would be consistent with the increased size of the asters in *APL10*/+ or *APL10* oocytes, raising the possibility that the asters contain γ-tubulin, as well as NcdGFP*.

Motor interactions with microtubules

The NcdNK motor binds more tightly than wild-type Ncd to microtubules in vitro (Song and Endow, 1998). To determine whether the mutant motor binds more tightly than wild type to spindle microtubules in live oocytes, we performed fluorescence loss in photobleaching (FLIP) experiments (Cole et al., 1996) by repeatedly scanning a defined region in a meiosis I spindle at high laser intensity (Supplementary material, Movies 5 and 6). Fluorescence loss over time was measured in scanned images to estimate a dissociation rate for the motor from spindle microtubules. The mean grey-level value of a region within the scanned area was determined over time and the values were plotted as a function of time. The data points were fit to a single exponential equation, $y=m_3+m_2*e^{(-m1*M0)}$, where y=grey-level value, M_0=time (seconds) and $y=m_3+m_2$ at $t=0$. The dissociation rate ($k_d=m_1$) for loss of fluorescence was obtained from the curve fit. The dissociation rate for oocytes containing two copies of the mutant *ncdNKgfp**

transgene was 0.042±0.005 second^{-1} (n=16). This was ~1.5-fold lower than the value of 0.065 ±0.005 second^{-1} (n=16) obtained for oocytes containing two copies of a wild-type *ncdgfp** (*M3M1*) transgene, indicating that the NcdNKGFP* motor binds more tightly than wild-type NcdGFP* to spindle microtubules in live cells. Plots of fluorescence loss over time for representative *ncdNKgfp** and *ncdgfp** meiosis I oocyte spindles are shown in Fig. 7.

Discussion

Nucleation of microtubules for spindle assembly is typically by centrosomes, which form asters at the poles and act as microtubule organizing and nucleating centers. However, some spindles lack centrosomes and asters. Classical examples are the anastral meiotic spindles of *Drosophila*, *Xenopus* and mouse oocytes. The mechanism by which anastral spindles form is poorly understood. Although significant advances have been made, including the first live imaging of meiosis I spindle assembly in *Drosophila* oocytes (Matthies et al., 1996) and the remarkable development of in vitro spindle assembly assays using *Xenopus* egg extracts (Heald et al., 1996), major questions remain regarding the assembly mechanism and proteins involved.

We showed previously that the minus-end spindle motor, Ncd, when expressed as a GFP fusion protein, binds to spindles of *Drosophila* oocytes and early embryos, and can be used to image spindle assembly during meiosis II and mitosis (Endow and Komma, 1997; Endow and Komma, 1998; Endow and Komma, 1996). The observation that Ncd does not bind to oocyte cytoplasmic microtubules (Hatsumi and Endow, 1992a; Matthies et al., 1996) led us to examine immature late stage 13 oocytes to determine whether we could follow germinal vesicle breakdown and meiosis I spindle assembly in *ncdgfp** oocytes. The studies reported here using NcdGFP* binding to meiotic spindle microtubules significantly extend the pioneering work of Matthies et al. (Matthies et al., 1996), who observed meiosis I spindle assembly in live wild-type and *cand* mutant oocytes by injecting rhodamine-tubulin into the oocytes prior to germinal vesicle breakdown. The use of NcdGFP* fluorescence to follow spindle assembly is an advance, as it is less disrupting to oocytes and much easier in terms of specimen preparation than performing the injections.

Assembly of anastral Drosophilaoocyte meiosis I spindles

Based on our analysis of meiosis I spindle assembly, we propose a model for assembly of anastral meiosis I spindles in *Drosophila* oocytes (Fig. 8). Following nuclear envelope breakdown, spindle assembly can be divided into seven phases: (1) formation of asters containing Ncd and microtubules; (2) migration of asters to the endobody; (3) microtubule nucleation at the endobody; (4) microtubule elongation in random directions; (5) bivalent association with microtubules; (6) lateral associations between bivalents owing to microtubule crosslinking; and (7) elongation into a bipolar spindle.

We attribute the initial event of microtubule nucleation to NcdGFP*-associated foci or asters that migrate towards the karyosome of condensed meiotic chromosomes, or endobody, and nucleate microtubules at the endobody. The specific mechanism by which microtubules are nucleated by the asters requires further work to elucidate. One possibility is that the Ncd motor crosslinks and bundles small microtubules, allowing them to serve as foci for microtubule growth. Nucleation at the endobody and outward growth implies that microtubule minus ends are associated with the chromosomes. The asters are larger in *ncdNKgfp** oocytes than in wild-type *ncdgfp** oocytes, presumably owing to tighter binding by the NcdNKGFP* motor to microtubules. The tighter binding by NcdNKGFP* than NcdGFP* to spindle microtubules in live oocytes was measured in FLIP experiments and is probably associated with increased bundling activity by the mutant motors, causing the asters to be larger. The asters are also larger in *APL10*/+ and *APL10* oocytes mutant for a γ-*Tub37C* allele that affects a residue that may be involved in lateral associations between γ-tubulin subunits, implying that the asters may

contain γ-tubulin as well as the NcdGFP* motor. γ- Tub37C has not been localized to developing *Drosophila* egg chambers or mature oocytes, despite several attempts (Matthies et al., 1996; Tavosanis et al., 1997) (H.N.S. and S.A.E., unpublished). Mutants of γ-Tub37C have been reported previously to disrupt oocyte meiosis I spindles (Tavosanis et al., 1997; Wilson and Borisy, 1998), although the abnormal meiotic figures in one of these studies may have been caused by inadvertent activation of the oocytes, based on their subsequently reported absence in ovulated oocytes or embryos (Llamazares et al., 1999). The role of γ-tubulin37C in meiosis I spindle assembly in *Drosophila* oocytes remains an open question that will probably require expression and careful analysis of a fluorescently labeled γ-tubulin protein to answer definitively.

In the work by Matthies et al. (Matthies et al., 1996), microtubule asters were occasionally observed but suggested not to have a role in spindle assembly. Visualization of asters by these workers after injection of rhodamine-tubulin supports our interpretation that the asters contain microtubules, as well as NcdGFP*. In this study we frequently saw multiple asters in close proximity to the germinal vesicle. One or more of these asters moved towards the endobody at the time of germinal vesicle breakdown and associated with it, after which spindle microtubules began to nucleate (Fig. 1). The timing of these events and the apparent nucleation of microtubules from the asters imply that the asters are involved in microtubule nucleation at the endobody, although further studies will be required to establish this.

A previous model for anastral spindle assembly, based on in vitro studies of spindle assembly around DNA-coated beads, proposes that microtubules nucleate at the chromatin with random polarity and form bundles of mixed polarity that undergo assortment and focusing to form a bipolar array (Heald et al., 1996). These workers suggested that microtubule nucleation is due to the influence of chromatin on the 'local state of the cytoplasm to favor microtubule nucleation and stabilization'. The model we present here differs from this previous study in that we propose that Ncd motor-associated asters migrate towards the chromosomes and nucleate microtubules, based on our observations in live *ncdgfp** oocytes. The bundled microtubules project in various orientations from the endobody and then undergo reorganization around the chromosomes in a manner similar to that proposed previously (Heald et al., 1996), except the chromosomes are the separated bivalents that subsequently interact laterally, presumably via motor-mediated microtubule crosslinking, to form a single bipolar array. Differences in the initial steps of microtubule nucleation may be species specific, but this possibility will require further study to establish.

The subsequent steps of bivalent chromosome association with microtubules and lateral association of the microtubule-coated chromosomes are reported here as intermediates in the assembly of an anastral spindle. Separated spindles associated with bivalent chromosomes were reported previously in *ncd* null mutant oocytes (Wald, 1936; Kimble and Church, 1983; Hatsumi and Endow, 1992b), but were interpreted to arise as a consequence of loss of microtubule crosslinking by the Ncd motor (Hatsumi and Endow, 1992a; Matthies et al., 1996) which caused them to detach from the spindle and become associated with microtubules, rather than disruption of an essential intermediate in the spindle assembly process. The previous lack of a complete pathway of meiosis I spindle assembly, including the initial steps of microtubule nucleation and intermediate steps that culminate in the appearance of a bipolar spindle, means that the effects of mutants could not be accurately determined. Here we present the first complete account of the assembly of an anastral spindle. We further separate the effects on spindle assembly of Ncd motility from the ability of the motor to hydrolyze ATP by analyzing an immobile mutant motor, *ncdNK*, and a severe loss-of-function mutant, ncd^2, which is probably defective in ATP hydrolysis. The effects of specific motor activities on spindle assembly have not been reported previously.

Ncd motor function in meiosis I spindle assembly

We tested the requirement for Ncd motility in meiosis I spindle assembly using a mutant motor, NcdNK, which is defective in microtubule gliding in vitro (Song and Endow, 1998). The NcdNK mutant motor binds microtubules to the coverslip, but does not move on microtubules in coverslip gliding assays. When assayed in vitro, the NcdNK mutant hydrolyzes ATP at the basal level, but shows no microtubule-stimulated ATPase activity and binds more tightly to microtubules than wild-type Ncd by ~two- to threefold. The mutant NcdNKGFP* motor showed a slower rate of release from spindle microtubules in the present study, indicating tighter binding to microtubules in live oocytes, although the increase over wild-type Ncd that we observed was less than in vitro, only ~1.5-fold. This may be due to the fact that the entire protein was present in the live oocytes, including the microtubule-binding tail region, whereas a truncated form of the motor that contained only the conserved motor domain was used in the in vitro biochemical assays. Nonetheless, our data show that the mutant NcdNKGFP* motor binds to microtubules more tightly than wild-type NcdGFP* in live cells, as well as in microtubule pelleting assays in vitro.

The NcdNKGFP* mutant motor is defective in meiosis I spindle assembly, primarily in maintaining stable lateral interactions between the microtubule-associated bivalent chromosomes. Lateral interactions between the bivalent chromosomes are probably due primarily to crosslinking of microtubules by the motor but also require motor movement along microtubules for stability, based on the effects of *ncdNKgfp**. The absence of stable lateral interactions prolongs or prevents bipolar spindle formation and causes the *ncdNKgfp** mutant oocytes to typically exhibit multiple or multipolar spindles. The abnormal spindles of the mutant indicate that the basal ATPase of the motor partially rescues spindle assembly, but Ncd motility is needed to stabilize lateral interactions of the chromosomes for bipolar spindle formation. Presumably, minus-end movement of wild-type Ncd along microtubules helps to hold the dynamically moving spindle-associated chromosomes together, which would otherwise move apart in the absence of a mobile Ncd motor. The requirement for Ncd motility in spindle assembly has not been demonstrated previously. Here, we separate the effects of motor movement on microtubules from microtubule binding by analysis of a mutant defective in motility, but not microtubule binding.

These conclusions from analysis of the *ncdNKgfp** mutant are supported by analysis of the more severe *ncd^{2}gfp** mutant, which is probably defective for both the motor basal and microtubule-stimulated ATPase, based on the nature of the mutation and its location in the motor domain (Endow and Komma, 1997). The *ncd^{2}gfp** mutant is defective in formation of lateral interactions between microtubule-associated bivalent chromosomes, which in turn affects pole formation and bipolar spindle assembly, causing them to be defective. Effects of the *cand* deletion mutant of *ncd* on pole formation in meiosis I spindles have been reported previously (Wald, 1936; Kimble and Church, 1983; Hatsumi and Endow, 1992b). The defect in an early step of the spindle assembly pathway greatly prolongs the process and prevents the appearance of normal bipolar spindles. The *ncd^{2}gfp** mutant is not defective in microtubule association with bivalent chromosomes, although the microtubules do not form a sheath around the chromosomes as in wild-type *ncdgfp** oocytes, indicating that hydrolysis of ATP by the motor may also be required for the motor to stabilize microtubule elongation. These effects of the Ncd^{2} motor could reflect the requirement for binding and releasing microtubules, which is thought to be coupled to the motor ATPase. A motor defective in ATPase activity could bind tightly to microtubules with both its microtubule-binding tail and motor domain during the initial stages of spindle assembly, and fail to release and rebind microtubules associated with an adjacent bivalent chromosome, blocking subsequent steps of assembly.

Our observations significantly extend those of Matthies and co-workers (Matthies et al., 1996), who reported the effects of *cand* as prolonging assembly of bipolar spindles and causing

spindles that did form to disorganize transiently and then reform. They inferred from these observations that microtubule bundling by the Ncd motor 'promotes assembly of a stable bipolar spindle', but did not identify the steps in the spindle assembly process that were defective, largely because the assembly pathway they reported was incomplete and lacked key initial and intermediate steps (Matthies et al., 1996). Based on our time-lapse analysis of live wild-type and mutant oocytes, we attribute the defects of the *ncd*^{2}*gfp** severe loss-of- function mutant to be at an early stage of spindle assembly: the formation of lateral interactions between microtubule-associated bivalent chromosomes and stabilization of elongating microtubules. The spindles we observed in *ncd*^{2}*gfp** mutant oocytes did not disassemble and reform as reported for *ca*nd (Matthies et al., 1996), although this may be a difference between the *ca*nd null mutant and *ncd*^{2}*gfp** loss-of-function mutant, in which a mutated Ncd motor capable of binding to spindle microtubules is expressed that may partially stabilize initial spindle structures.

Both of the *ncd* mutants we examined in this study express defective Ncd motor proteins, whereas mutant *ca*nd oocytes produce no Ncd protein but can assemble abnormal multipolar meiotic spindles (Kimble and Church, 1983; Hatsumi and Endow, 1992b; Matthies et al., 1996), requiring a much longer time (Matthies et al., 1996). These results indicate that there is a dominant pathway of meiosis I spindle assembly in *Drosophila* oocytes that depends on the Ncd motor. In the absence of Ncd, spindles can initiate assembly, but the process is much less efficient. Initiation of microtubule nucleation may eventually occur by chance encounters of small microtubules with the karyosome, rather than being facilitated in their association by the Ncd motor. Assembly is then blocked or destabilized at an early step of the pathway, resulting in abnormal spindles. This parallels findings for mitotic spindle assembly in *C. elegans*, which depends on γ-tubulin, and fails in its absence or loss of function (Hannak et al., 2002). The findings we present here define a pathway for anastral spindle assembly, including key features of the process: microtubule nucleation at the chromosomes, formation of microtubule-associated bivalent chromosomes and their lateral association into a bipolar spindle, and identify the steps dependent on Ncd motility and ability to hydrolyze ATP. This pathway provides an essential framework for further analysis of the assembly process and the proteins involved.

Supplementary Material

Refer to Web version on PubMed Central for supplementary material.

Acknowledgements

We thank C. Berg for help with oocyte staging and culture, and confocal microscopy, and W. Sullivan for a generous gift of rhodamine-conjugated anti-α-tubulin antibody. Supported by grants from the NIH and HFSP to S.A.E. and the Swedish Royal Academy of Science to H.N.S.

References

Brent AE, MacQueen A, Hazelrigg T. The Drosophila *wispy* gene is required for RNA localization and other microtubule-based events of meiosis and early embryogenesis. Genetics 2000;154:1649–1662. [PubMed: 10747060]

Carabatsos MJ, Combelles CM, Messinger SM, Albertini DF. Sorting and reorganization of centrosomes during oocyte maturation in the mouse. Microsc Res Tech 2000;49:435–444. [PubMed: 10842370]

Clarkson M, Saint R. A His2AvDGFP fusion gene complements a lethal His2AvD mutant allele and provides an in vivo marker for Drosophila chromosome behavior. DNA Cell Biol 1999;18:457–462. [PubMed: 10390154]

Cole NB, Smith CL, Sciaky N, Terasaki M, Edidin M, Lippincott-Schwartz J. Diffusional mobility of Golgi proteins in membranes of living cells. Science 1996;273:797–801. [PubMed: 8670420]

Combelles CM, Albertini DF. Microtubule patterning during meiotic maturation in mouse oocytes is determined by cell cycle-specific sorting and redistribution of γ-tubulin. Dev Biol 2001;239:281–294. [PubMed: 11784035]

Cullen CF, Ohkura H. Msps protein is localized to acentrosomal poles to ensure bipolarity of *Drosophila* meiotic spindles. Nature Cell Biol 2001;3:637–642. [PubMed: 11433295]

Davis I, Girdham CH, O'Farrell PH. A nuclear GFP that marks nuclei in living *Drosophila* embryos; maternal supply overcomes a delay in the appearance of zygotic fluorescence. Dev Biol 1995;170:726–729. [PubMed: 7649398]

Desai A, Maddox PS, Mitchison TJ, Salmon ED. Anaphase A chromosome movement and poleward spindle microtubule flux occur at similar rates in *Xenopus* extract spindles. J Cell Biol 1998;141:703–713. [PubMed: 9566970]

Dorman JB, James KE, Fraser SE, Kiehart DP, Berg CA. *bullwinkle* is required for epithelial morphogenesis during *Drosophila* oogenesis. Dev Biol 2004;267:320–341. [PubMed: 15013797]

Doxsey SJ, Stein P, Evans L, Calarco PD, Kirschner M. Pericentrin, a highly conserved centrosome protein involved in microtubule organization. Cell 1994;76:639–650. [PubMed: 8124707]

Endow SA. Microtubule motors in spindle and chromosome motility. Eur J Biochem 1999;262:12–18. [PubMed: 10231358]

Endow SA, Komma DJ. Centrosome and spindle function of the *Drosophila* Ncd microtubule motor visualized in live embryos using Ncd-GFP fusion proteins. J Cell Sci 1996;109:2429–2442. [PubMed: 8923204]

Endow SA, Komma DJ. Spindle dynamics during meiosis in *Drosophila* oocytes. J Cell Biol 1997;137:1321–1336. [PubMed: 9182665]

Endow SA, Komma DJ. Assembly and dynamics of an anastral:astral spindle: the meiosis II spindle of *Drosophila* oocytes. J Cell Sci 1998;111:2487–2495. [PubMed: 9701548]

Foe, V. E., Odell, G. M. and Edgar, B. A. (1993). Mitosis and morphogenesis in the *Drosophila* embryo: point and counterpoint. In *The Development of Drosophila melanogaster*, vol. I (eds M. Bate and A. M. Arias), pp. 149–300. Cold Spring Harbor, NY: Cold Spring Harbor Laboratory Press.

Grell RF. A new hypothesis on the nature and sequence of meiotic events in the female of Drosophila melanogaster. Proc Natl Acad Sci USA 1962;48:165–172. [PubMed: 13901696]

Grell RF. Distributive pairing: the size-dependent mechanism for regular segregation of the fourth chromosomes in Drosophila melanogaster. Proc Natl Acad Sci USA 1964;52:226–232. [PubMed: 14206584]

Gueth-Hallonet C, Antony C, Aghion J, Santa-Maria A, Lajoie-Mazenc I, Wright M, Maro B. γ-Tubulin is present in acentriolar MTOCs during early mouse development. J Cell Sci 1993;105:157–166. [PubMed: 8360270]

Hannak E, Oegema K, Kirkham M, Gönczy P, Habermann B, Hyman AA. The kinetically dominant assembly pathway for centrosomal asters in Caenorhabditis elegans is γ-tubulin dependent. J Cell Biol 2002;157:591–602. [PubMed: 12011109]

Hatsumi M, Endow SA. The *Drosophila* ncd microtubule motor protein is spindle-associated in meiotic and mitotic cells. J Cell Sci 1992a;103:1013–1020. [PubMed: 1487485]

Hatsumi M, Endow SA. Mutants of the microtubule motor protein, nonclaret disjunctional, affect spindle structure and chromosome movement in meiosis and mitosis. J Cell Sci 1992b;101:547–559. [PubMed: 1522143]

Heald R, Tournebize R, Blank T, Sandalzopoulos R, Becker P, Hyman A, Karsenti E. Self-organization of microtubules into bipolar spindles around artificial chromosomes in *Xenopus* egg extracts. Nature 1996;382:420–425. [PubMed: 8684481]

Heim R, Cubitt AB, Tsien RY. Improved green fluorescence. Nature 1995;373:663–664. [PubMed: 7854443]

Hunter AW, Wordeman L. How motor proteins influence microtubule polymerization dynamics. J Cell Sci 2000;113:4379–4389. [PubMed: 11082031]

Inoué S, Salmon ED. Force generation by microtubule assembly/disassembly in mitosis and related movements. Mol Biol Cell 1995;6:1619–1640. [PubMed: 8590794]

Karsenti E, Vernos I. The mitotic spindle: a self-made machine. Science 2001;294:543–547. [PubMed: 11641489]

Kimble M, Church K. Meiosis and early cleavage in *Drosophila melanogaster* eggs: effects of the claret-non-disjunctional mutation. J Cell Sci 1983;62:301–318. [PubMed: 6413518]

Komma DJ, Horne AS, Endow SA. Separation of meiotic and mitotic effects of *claret nondisjunctional* on chromosome segregation in *Drosophila.* EMBO J 1991;10:419–424. [PubMed: 1825056]

Lawrence CJ, Dawe RK, Christie KR, Cleveland DW, Dawson SC, Endow SA, Goldstein LSB, Goodson HV, Hirokawa N, Howard J, et al. A standardized kinesin nomenclature. J Cell Biol 2004;167:19–22. [PubMed: 15479732]

Lee J, Miyano T, Moor RM. Spindle formation and dynamics of gamma-tubulin and nuclear mitotic apparatus protein distribution during meiosis in pig and mouse oocytes. Biol Reprod 2000;62:1184–1192. [PubMed: 10775165]

Lee MJ, Gergely F, Jeffers K, Peak-Chew SY, Raff JW. Msps/XMAP215 interacts with the centrosomal protein D-TACC to regulate microtubule behaviour. Nat Cell Biol 2001;3:643–649. [PubMed: 11433296]

Llamazares S, Tavosanis G, Gonzalez C. Cytological characterization of the mutant phenotypes produced during early embryogenesis by null and loss-of-function alleles of the γ*Tub37C* gene in *Drosophila.* J Cell Sci 1999;112:659–667. [PubMed: 9973601]

Matthies HJG, McDonald HB, Goldstein LSB, Theurkauf WE. Anastral meiotic spindle morphogenesis: role of the Non-Claret Disjunctional kinesin-like protein. J Cell Biol 1996;134:455–464. [PubMed: 8707829]

Mitchison TJ, Salmon ED. Mitosis: a history of division. Nat Cell Biol 2001;3:17–21.

Nogales E, Wolf SG, Downing KH. Structure of the αβ tubulin dimer by electron crystallography. Nature 1998;391:199–203. [PubMed: 9428769]

Novitski E. An alternative to the distributive pairing hypothesis in Drosophila. Genetics 1964;50:1449–1451. [PubMed: 14239803]

O'Tousa J, Szauter P. The initial characterization of non-claret disjunctional (ncd): evidence that ca^{nd} is the double mutant, ca ncd. Dros Inf Serv 1980;55:119.

Riparbelli MG, Callaini G. Meiotic spindle organization in fertilized *Drosophila* oocyte: presence of centrosomal components in the meiotic apparatus. J Cell Sci 1996;109:911–918. [PubMed: 8743938]

Riparbelli MG, Callaini G. γ-Tubulin is transiently associated with the Drosophila oocyte meiotic apparatus. Eur J Cell Biol 1998;75:21–28. [PubMed: 9523151]

Schüpbach T, Wieshaus E. Female sterile mutations on the second chromosome of *Drosophila melanogaster*. I Maternal effect mutations. Genetics 1989;121:101–117. [PubMed: 2492966]

Sharp DJ, Brown HM, Kwon M, Rogers GC, Holland G, Scholey JM. Functional coordination of three mitotic motors in *Drosophila* embryos. Mol Biol Cell 2000;11:241–253. [PubMed: 10637305]

Song H, Endow SA. Decoupling of nucleotide- and microtubule-binding in a kinesin mutant. Nature 1998;396:587–590. [PubMed: 9859995]

Sonnenblick, B. P. (1950). The early embryology of Drosophila melanogaster. In *Biology of Drosophila* (ed. M. Demerec), pp. 62–167. New York, NY: Hafner.

Surrey T, Nedelec F, Leibler S, Karsenti E. Physical properties determining self-organization of motors and microtubules. Science 2001;292:1167–1171. [PubMed: 11349149]

Szollosi D, Calarco P, Donahue RP. Absence of centrioles in the first and second meiotic spindles of mouse oocytes. J Cell Sci 1972;11:521–541. [PubMed: 5076360]

Tavosanis G, Llamazares S, Goulielmos G, Gonzalez C. Essential role for γ-tubulin in the acentriolar female meiotic spindle of *Drosophila.* EMBO J 1997;16:1809–1819. [PubMed: 9155007]

Theurkauf WE, Hawley RS. Meiotic spindle assembly in *Drosophila* females: behavior of nonexchange chromosomes and the effects of mutations in the nod kinesin-like protein. J Cell Biol 1992;116:1167–1180. [PubMed: 1740471]

Wald H. Cytologic studies on the abnormal development of the eggs of the claret mutant type of Drosophila simulans. Genetics 1936;21:264–281. [PubMed: 17246793]

Waterman-Storer CM, Desai A, Bulinski JC, Salmon ED. Fluorescent speckle microscopy, a method to visualize the dynamics of protein assemblies in living cells. Curr Biol 1998;8:1227–1230. [PubMed: 9811609]

Wilson, E. B. (1934). The Cell in Development and Heredity. New York, NY: Macmillan.

Wilson PG, Borisy GG. Maternally expressed γTub37CD in *Drosophila* is differentially required for female meiosis and embryonic mitosis. Dev Biol 1998;199:273–290. [PubMed: 9698447]

Yamamoto AH, Komma DJ, Shaffer CD, Pirrotta V, Endow SA. The *claret* locus in *Drosophila* encodes products required for eyecolor and for meiotic chromosome segregation. EMBO J 1989;8:3543–3552. [PubMed: 2479546]

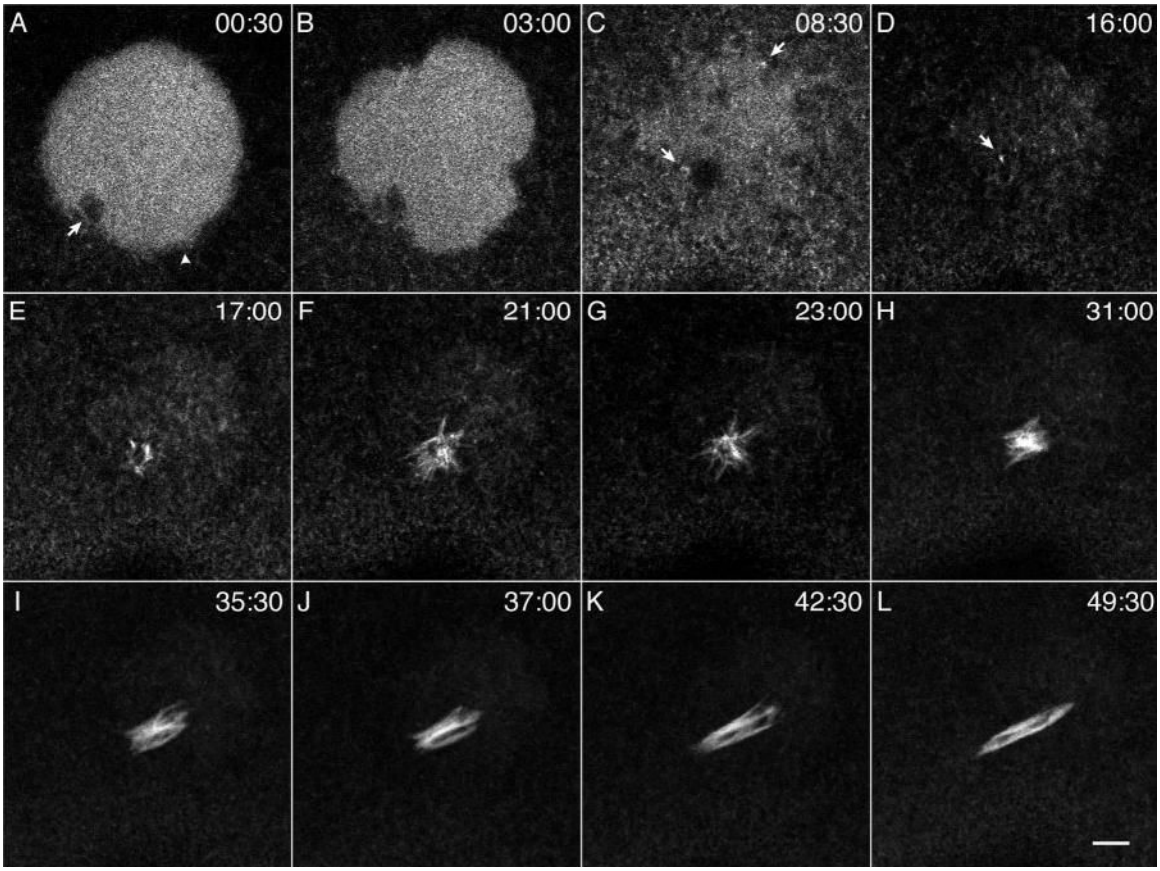

Fig. 1.

Meiosis I spindle assembly in a wild-type *ncdgfp** oocyte. Images from a time-lapse sequence (Movie 1 in supplementary material) show the steps of spindle assembly in a live oocyte. (A,B) Germinal vesicle breakdown. The margin of the nuclear envelope shows regions of unevenness (arrowhead). The dark spot in the germinal vesicle (arrow) is the karyosome of condensed chromosomes, or endobody. (C,D) Dispersion of the germinal vesicle contents into the ooplasm. The arrows indicate the microtubule foci or asters, one of which is associated with the endobody. (E–G) Nucleation of randomly oriented microtubules at the endobody. (H) Differentiation of the endobody into microtubule-associated bivalent chromosomes. (I) Formation of lateral interactions between microtubule-associated chromosomes. (J–L) Formation and elongation of a bipolar spindle. Time, minutes:seconds. Bar, 5 μm.

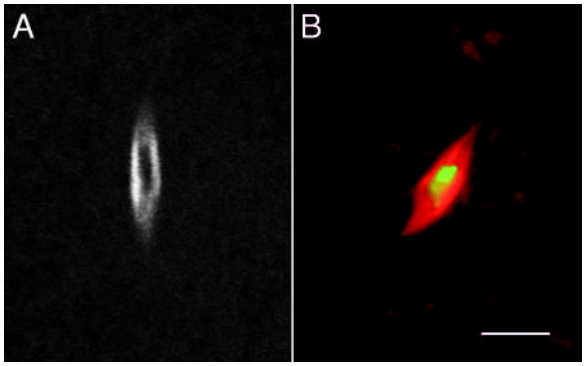

Fig. 2.

Chromosomes in the meiosis I spindle. The chromosomes in live oocytes were confirmed by comparing fixed and stained oocytes. (A) Mature spindle in a live *ncdgfp** oocyte. The dark region in the center of the spindle excludes NcdGFP* and was inferred to correspond to the condensed meiotic chromosomes. (B) Wild-type oocyte (Oregon R) fixed and stained with rhodamine-labeled anti-α-tubulin antibody (red) and DAPI (green). The small dots at the distal ends of the chromosome mass are the small 4th chromosomes. Bar, 5 μm.

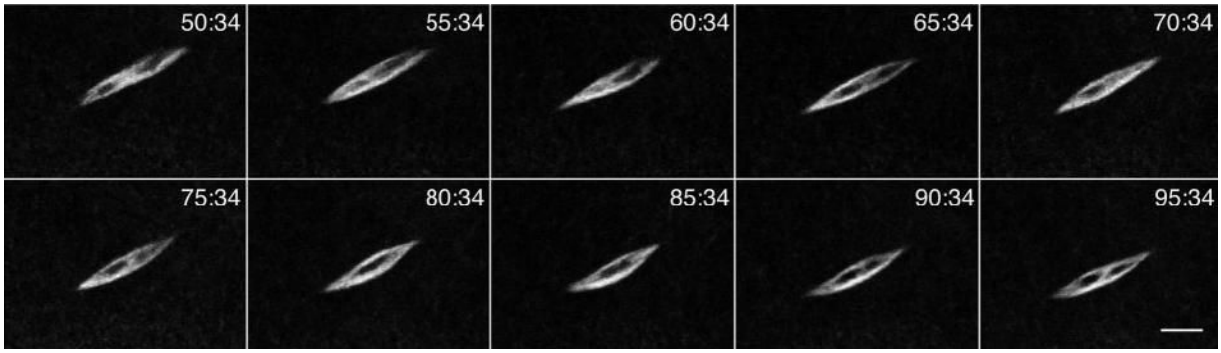

Fig. 3.

Movement of chromosomes following meiosis I spindle assembly. Time-lapse images of the same oocyte as in Fig. 1, shown at 5 minute intervals for 45 minutes following the appearance of a polar spindle (see Movie 2 in supplementary material). The dark regions, interpreted to be the meiotic chromosomes, continue moving in the spindle. Time, minutes:seconds. Bar, 5 μm.

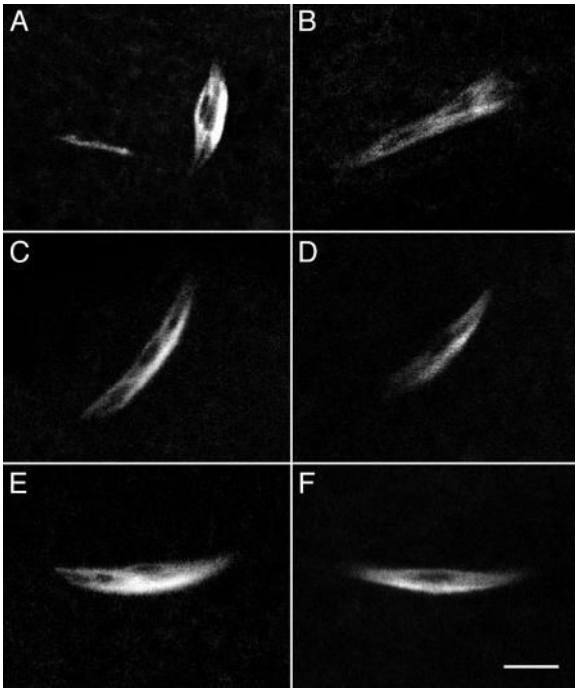

Fig. 4.
Meiosis I spindles in *ncdNKgfp** mutant oocytes. (A) Split spindle with a separated microtubule-associated chromosome. (B) Split, multipolar spindle. (C-E) Partially fused or side-by-side spindles. (F) Apparently normal spindle. Bar, 5 μm.

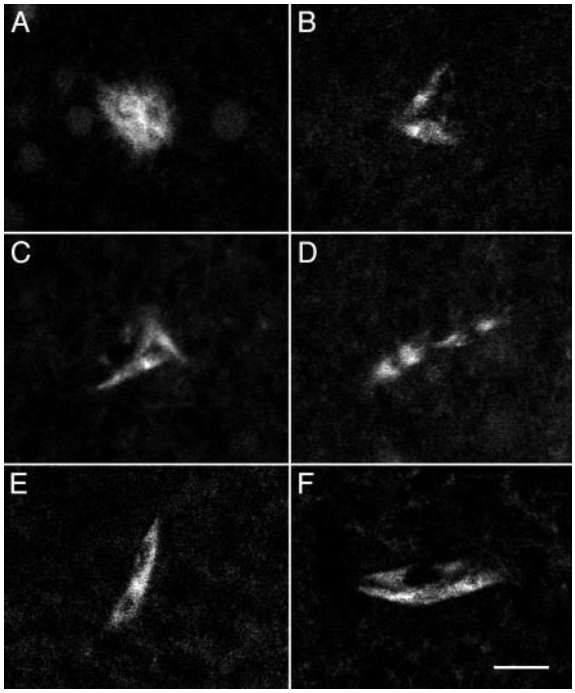

Fig. 5.
Meiosis I spindles in *ncd*^{2}*gfp** mutant oocytes. (A) Immature spindle. (B-F) Immature, multipolar, or multiple spindles. Bar, 5 μm.

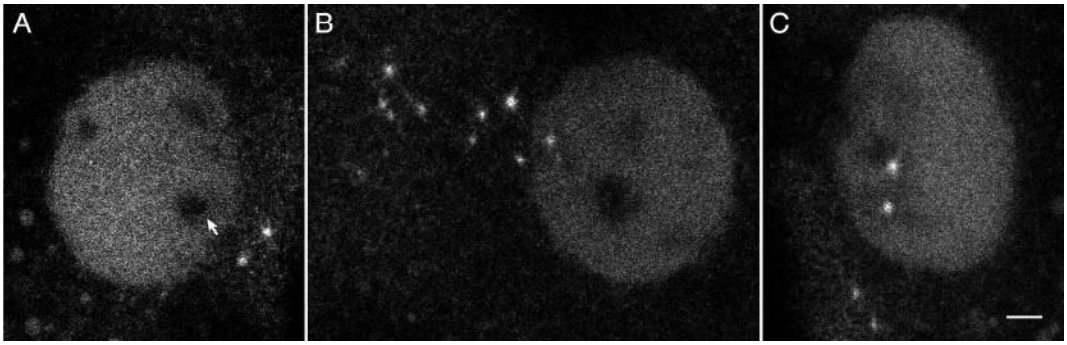

Fig. 6.

Ncd motor-associated asters at the germinal vesicle. (A) Two large fluorescent asters just outside the germinal vesicle of an *ncdNKgfp** oocyte. The karyosome or endobody (arrow), around which microtubule nucleation occurred, is the dark body to the lower right, closest to the fluorescence foci. The other two dark regions are due to uneven dispersion of germinal vesicle contents into the ooplasm. (B) A cluster of large asters near the germinal vesicle of an *ncdNKgfp** oocyte. (C) Two large asters in the germinal vesicle of an *APL10*/+ oocyte; two more large asters are in the ooplasm. The fluorescent asters migrate towards the karyosome of condensed chromosomes and nucleate microtubules at germinal vesicle breakdown. The asters are larger in *ncdNKgfp** and *APL10*/+ or *APL10* oocytes, than wild-type *ncdgfp** oocytes (see Fig. 1C,D for comparison). Bar, 5 μm.

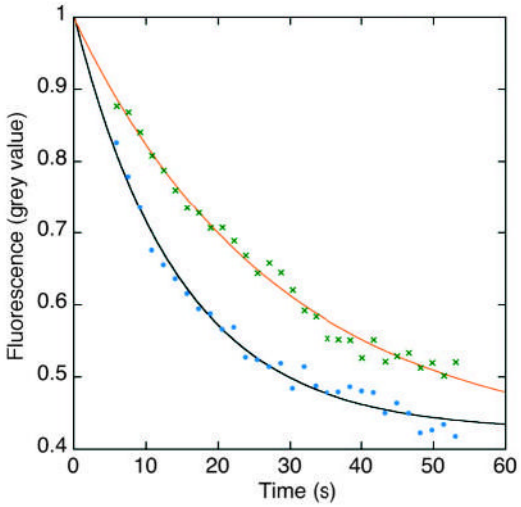

Fig. 7.

Binding by the NcdNKGFP* motor to meiosis I spindle microtubules. The dissociation rate (k_d) of the motor from microtubules was estimated for NcdNKGFP* and wild-type NcdGFP* using fluorescence loss in photobleaching (FLIP) experiments. Plots of fluorescence (grey value) as a function of time (s, seconds) were fitted to a single exponential curve to estimate the k_d. Representative plots are shown for NcdNKGFP* (crosses and red line, k_d=0.035 second^{-1}) and wild-type NcdGFP* (filled circles and black line, k_d=0.069 second^{-1}). The mean k_d for NcdNKGFP* was 0.042±0.005 second^{-1} (n=16) and that for wild-type NcdGFP* was 0.065±0.005 second^{-1} (n=16). Curves are normalized to a starting grey level of 1.000 for comparison.

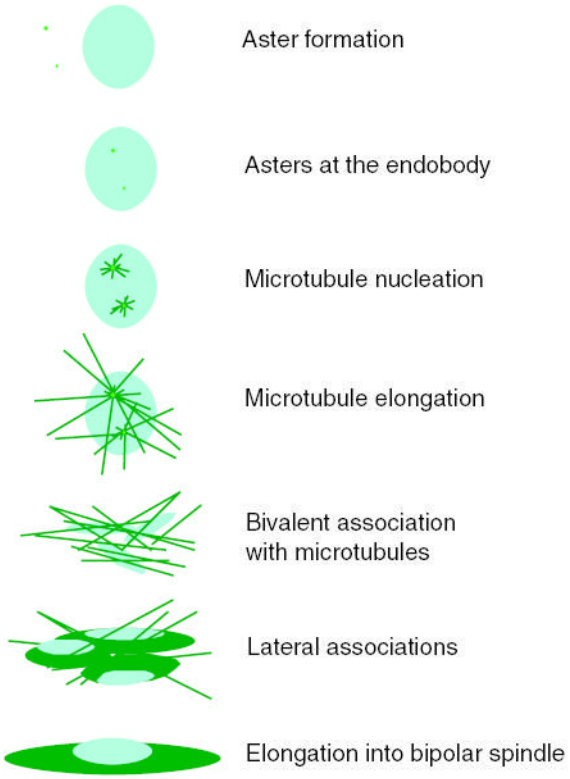

Fig. 8.

Assembly of anastral *Drosophila* oocyte meiosis I spindles. The model shows seven steps that lead to anastral spindle assembly, based on observation of spindle assembly in live wild-type *ncdgfp** oocytes. The blue body represents the karyosome of condensed meiotic chromosomes, or endobody, at which microtubule nucleation is initiated.

Table 1

Kinetics of meiosis I spindle assembly

Transgene	End of GVB Time (minutes)	MT nucleation Time (minutes)	Lateral interactions Time (minutes)	Bipolar spindle Time (minutes)	MT nucleation to bipolar spindle Time (minutes)	Oocytes *n*
*ncdgfp*ca*nd	0	9.9±1.3	22.4±2.9	40.0±1.6	29.4±1.6	10
*ncdNKgfp*ca*nd	0	9.9±3.8[*]	>33.1±10.2[†]	>63.2± 5.9	>48.6 ± 1.1	5
*ncd2gfp*ca*nd	0	12.8±1.8	>95.6±22.9	>129.5±9.9[‡]	>116.7±10.8[‡]	5

Times (mean ± s.e.m.) are given following the end of germinal vesicle breakdown (GVB), except for those in the column labeled 'MT nucleation to bipolar spindle'. MT, microtubule.

[*] The time of microtubule nucleation could not be determined for one oocyte.

[†] Lateral interactions were not observed in one oocyte.

[‡] Normal bipolar spindles were not observed; times are the mean time of observation following GVB or MT nucleation.

Table 2

Genetic tests of the *ncdNKgfp** transgene

Female parent	Total embryos *n*	Total adults *n*	Embryo viability Frequency	Gametic ND + loss Frequency	Zygotic loss Frequency
ncdgfp ca*nd	3480	3235	0.930	0.006	<0.001
ncdNKgfp ca*nd/+	1751	1382	0.789	0.001	0.001
ncdNKgfp ca*nd	3598	349	0.097	0.138	0.040
cand	1277	144	0 113	0.238	0.056

Offspring from matings of indicated parental females to tester males. Data for *ncdgfp* (M3M1; M9F1) ca*nd females were from Endow and Komma (1996), and those for *ca*nd females were from Endow and Komma (1997) ND, nondisjunction.